Short-term Aluminum Administration in the Rat

Effects on Bone Formation and Relationship to Renal Osteomalacia

William G. Goodman, Jeanenne Gilligan, and Ronald Horst
Medical and Research Services, Sepulveda Veterans Administration Medical Center, University of California, Los Angeles/San Fernando Valley Program, Sepulveda, California 91343; National Animal Disease Center, Agriculture Research Science and Education Administration, United States Department of Agriculture, Ames, Iowa, 50010

Abstract. Aluminum may be pathogenic in the osteomalacia observed in some patients receiving hemodialysis. To study the early effects of Al on bone growth, bone formation, mineralization, and resorption were measured during short-term Al exposure in the tibial cortex of pair-fed control (C, n = 10), aluminum-treated (AL, n = 9), subtotally nephrectomized control (NX-C, n = 7), and subtotally nephrectomized aluminum-treated (NX-AL, n = 8) rats using double tetracycline labeling of bone. Animals received 2 mg/d of elemental Al intraperitoneally for 5 d/wk over 4 wk. Total bone and matrix (osteoid) formation, periosteal bone and matrix formation, and periosteal bone and matrix apposition fell by 20% in AL from C, $P < 0.05$ for all values, and by 40% in NX-AL from NX-C, $P < 0.01$ for all values. Moreover, each measurement was significantly less in NX-AL than in AL, $P < 0.05$ for all values. Osteoid width did not increase following aluminum administration in either AL or NX-AL. Resorption surface increased from control values in both AL and NX-AL; also, resorptive activity at the endosteum was greater in NX-AL than in NX-C, $P < 0.05$. Thus, aluminum impairs new bone and matrix formation but does not cause classic osteomalacia in the cortical bone of rats whether renal function is normal or reduced. These findings may represent either a different response to aluminum administration in cortical bone as contrasted to trabecular bone or an early phase in the development of osteomalacia. Aluminum may increase bone resorption and contribute to osteopenia in clinical states associated with aluminum accumulation in bone.

Received for publication 20 June 1983 and in revised form 26 August 1983.

The Journal of Clinical Investigation, Inc.
Volume 73, January 1984, 171–181

Introduction

Aluminum accumulation in bone may be a factor in the pathogenesis of dialysis-associated osteomalacia (1–8). The aluminum content of bone has been shown to be increased by both chemical and histochemical techniques in some patients undergoing hemodialysis, a substantial portion of whom show histologic evidence of osteomalacia on bone biopsy (6–9). The severity of osteomalacia in these patients, assessed by quantitative histomorphometry, correlates positively with the content of aluminum in bone (9). Furthermore, the findings of one clinical investigation suggest that aluminum deposition in bone may antedate overt osteomalacic changes in patients receiving hemodialysis (7). Aluminum may therefore interfere with normal bone turnover and mineralization. Alternatively, the passive binding of aluminum by unmineralized bone matrix, i.e., osteoid, could account for the associations described. Since the kidney is the primary route for the excretion of aluminum, it is not unexpected that individuals with impaired renal function would be predisposed to the retention of aluminum in various tissues (10, 11).

Few experimental investigations have examined the issue of aluminum toxicity in the pathogenesis of osteomalacia. Ellis et al. (12) described a defect in the mineralization of newly formed bone at the tibial epiphyses of rats given aluminum; this was reversed when the administration of aluminum was stopped. Two other reports have also suggested that aluminum administration can induce osteomalacia in the trabecular bone of rats with renal insufficiency (13–14). However, the results of these studies, as well as observations from our laboratory, indicate that rats given daily intraperitoneal injections of aluminum chloride exhibit less weight gain and slower bone growth than saline-injected control animals. These differences in animal growth must be adequately controlled if more direct comparisons of the effects of aluminum on bone are to be made. Since the

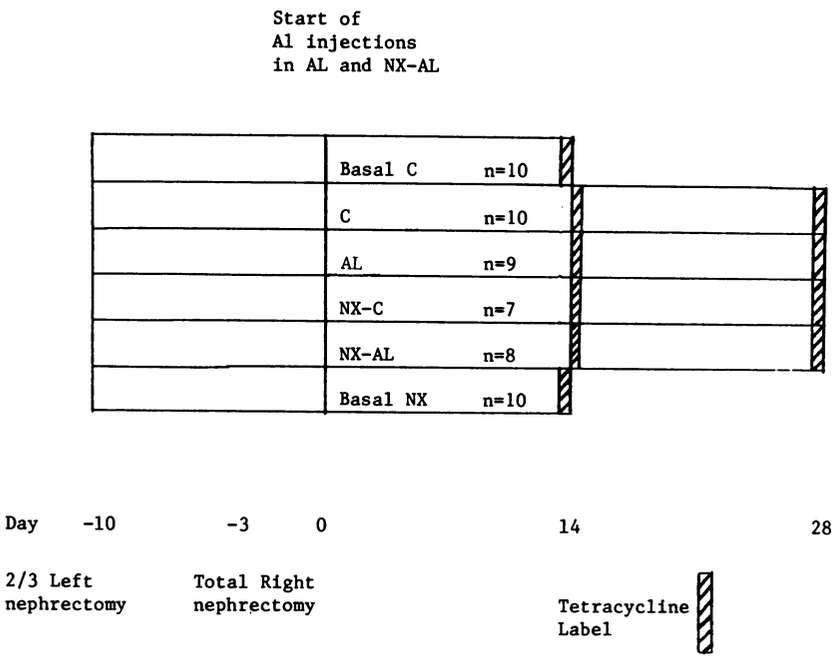

Figure 1. Experimental protocol.

duration of study in previous reports has been 8 wk or longer, little is known about the early effects of aluminum administration on bone growth or bone histology. Moreover, data from clinical investigations of dialysis osteomalacia and from in vivo and in vitro experimental work suggest that aluminum may alter the metabolism of vitamin D and the secretion of parathyroid hormone (15–17); such changes may contribute to the skeletal findings reported during long-term exposure to aluminum.

The present study was undertaken (*a*) to distinguish between a general effect of aluminum administration on animal growth and a more specific effect on bone growth, (*b*) to examine the manifestations of aluminum loading on bone histology and bone growth during short-term, i.e., 4 wk, aluminum exposure, and (*c*) to evaluate the role of renal insufficiency in mediating the skeletal effects of aluminum. Cortical bone was examined by using a well-established model of quantitative bone histology and growth in the rat.

Methods

Experimental design. 60 weanling, male Holtzman rats were obtained at 21 d of age. One half of the animals underwent a two-stage, subtotal nephrectomy before study (Fig. 1). The first stage nephrectomy was done 10 d before the start of the experimental period by removing two-thirds of the left kidney, after ligating both the upper and lower poles, under pentobarbital anesthesia (20 mg/kg); this was followed 1 wk later by a total right nephrectomy 3 d before the experimental period.

Six groups of 10 rats each, four final and two basal, were studied (Fig. 1). Rats with intact renal function were assigned at random to one of three groups: control (C),[1] aluminum-treated (AL), or basal control (Basal-C). Likewise, subtotally nephrectomized animals were randomly allocated to one of the three remaining groups: nephrectomized control (NX-C), nephrectomized aluminum-treated (NX-AL), or basal nephrectomized (Basal-NX). All rats were housed in individual metabolic cages with free access to water and maintained on standard rat chow (Ralston Purina Co., Chicago, IL) containing 0.6% calcium and 0.6% phosphorus for the remainder of the study. To assure comparable weight gain and body growth among all six groups, rats within each group were ranked by weight at the start of the experiment; animals of corresponding rank from each group were given an equal amount of food daily throughout the study.

Rats from each final group, C, AL, NX-C, and NX-AL, were maintained for 4 wk and killed on day 28 at the conclusion of the experiment. Bone growth was measured in these animals during the final 2 wk of study by using double tetracycline labeling of bone (18). Animals in each of the two basal groups, Basal-C and Basal-NX, were killed on day 14; the measurements made in these basal rats are discussed in detail subsequently (see below).

One group of rats with normal renal function (AL) and one group of subtotally nephrectomized rats (NX-AL) received intraperitoneal injections of $AlCl_3$ in saline vehicle 5 d/wk for a total of 4 wk. During the first week of study, animals were given an incremental dose of aluminum (Al) to avoid the development of chemical peritonitis; subsequently, the dose of elemental Al was 2 mg per day. The 4-wk cumulative dose of Al was 34.2 mg/rat. Control rats (C and NX-C) and basal rats (Basal-C and Basal-NX) received intraperitoneal vehicle only for 5 d each week until death. After death the left tibia from all rats was removed, stripped of adhering soft tissue, and placed in gauze saturated with 10% buffered formalin until sectioning.

Bone measurements. Bone growth was measured over a 14-d period at the tibial diaphysis in rats from the four final groups using double

1. *Abbreviations used in this paper:* AL, aluminum-treated; Basal-C, basal control; Basal-NX, basal nephrectomized; C, control; iPTH, immunoreactive PTH; NX-AL, nephrectomized aluminum-treated; NX-C, nephrectomized control; PTH, parathyroid hormone; $1,25(OH)_2D$, 1,25-dihydroxyvitamin D; 25(OH)D, 25-hydroxyvitamin D.

tetracycline labeling of bone according to the model described by Baylink et al. (19). Animals in Basal-C and Basal-NX received a single dose of tetracycline HCl, 20 mg/kg, 24 h before death on day 14 (Fig. 1). At the time of death of the two basal groups, rats in each of the four final groups were given an injection of tetracycline marking the start of the bone labeling period; a second tetracycline label was administered 24 h before death on day 28 at the end of the experiment.

All histologic measurements were done on cross-sections of the tibial diaphysis taken from the segment immediately proximal to the fibular junction by using a circular saw (Buehler Isomet, Buehler Ltd., Evanston, IL). The bone was oriented such that all sections were made perpendicular to the longitudinal axis. Three consecutive 35-μm sections were obtained; these were hand-ground to a thickness of 10–15 μm, stained with nuclear fast red, dehydrated in acetone, cleared in xylene, and mounted in Pro-Texx (Lerner Laboratories) for quantitative histological measurements as previously reported (19). This staining procedure permits differentiation between unmineralized osteoid and adjacent mineralized bone. Our laboratory has confirmed previous work (19) which documents that the values for the histologic variables determined from each of three consecutive sections of the tibia at this site are comparable; therefore, each section is representative of the entire sampling site. Since the length of the tibial sampling site from which the sections of bone were taken was >1 mm, the calculated rates of bone formation and resorption were expressed in units of volume per unit time (19).

Quantitative histologic measurements were done with a digitizer tablet (Summagraphics Corp., Fairfield, CT) interfaced with a microcomputer (IBM PC, IBM Instruments, IBM Corp., Danbury, CT) and a series of measuring programs. Light microscopy was done with both halogen and tungsten light sources; image projection was accomplished using a projection prism (× 120), and a drawing tube (× 130) attached to a Leitz Dialux microscope (Leitz, Wetzlar, Federal Republic of Germany). Fluorescent microscopy (× 930) was done using a 200-W mercury light source in conjunction with a Ploemo-Pak (Leitz) epifluorescent microscope attachment.

The histologic variables measured in rats killed at the end of the experiment are illustrated in the left panel of Fig. 2; those determined in basal rats are shown in the right panel. All values for length and area represent the mean of duplicate determinations in individual rats. Periosteal- and endosteal-forming surfaces were identified by the presence of both an osteoid seam and an adjacent band of tetracycline fluorescence. The length of the endosteal resorption surface was determined from the difference between the lengths of the total and the endosteal-forming surfaces (19). Width measurements at the periosteum were done at 60° intervals along the circumference of this surface, and the results represent the mean of these six determinations. Endosteal widths were measured at frequent and equal intervals along the length of the endosteal surface by using a minimum of 15 determinations per section. The results for endosteal width represent the mean of these multiple measurements (19). The values for width, derived in this manner, were used in subsequent calculations of bone growth for individual rats. (See Appendix).

The calculations used to determine dynamic bone histomorphometry require the measurement of histologic variables at the start and at the end of the bone labeling period. The variables shown in the right panel of Fig. 2 cannot be measured from sections of bone obtained at the end of the experiment. Thus, the histologic measurements from each of the two basal groups were taken to represent the status of the bone at the beginning of the labeling period for rats from the corresponding final groups. For C and AL, the corresponding basal group was Basal-C; for NX-C and NX-AL, it was Basal-NX (Fig. 1). The assignment of measurements made in individual basal rats to rats from the final groups for purposes of calculation was made on the basis of a ranking procedure (19) whereby basal rats were ranked in descending order by the size of the endosteal area, and final rats by the size of the initial endosteal area.

The calculations used to determine bone growth at this site in the rat tibia, and the validation of these methods, have been reported in detail elsewhere (19); a brief summary of these calculations is presented in Appendix.

Serum and urine determinations. 24-h urine collections were made on days 25 and 26 of the experimental period, 2 and 3 d, respectively, before termination of the study. Aliquots of urine were saved for subsequent analysis. Blood was obtained just before death by cardiac puncture under anesthesia and serum was preserved. The concentrations of calcium in serum and urine were determined by atomic absorption spectroscopy (20), of phosphorus in serum and urine by colorimetric method (21), and of creatinine in serum and urine by modified Jaffe method (22). Serum levels of 25-hydroxyvitamin D (25[OH]D) and 1,25-dihydroxyvitamin D (1,25$[OH]_2$D) were measured by methods described previously

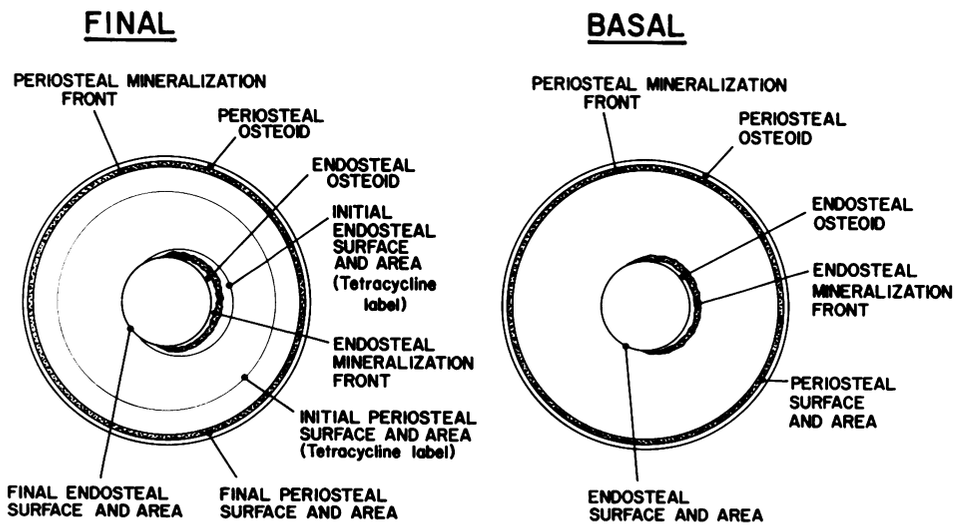

Figure 2. A diagrammatic representation of a cross-section of the tibial diaphysis of a rat from which histologic measurements of cortical bone are made. The variables measured in final rats are shown in the left panel and those measured in basal rats in the right panel. Initial lengths and areas are determined from tetracycline labels in rats from the final groups.

Table I. Weight Gain, Renal Function, and Serum Biochemical Values in Control and AL Rats

	Basal-C (n = 10)	C (n = 10)	AL (n = 9)	Basal-NX (n = 10)	NX-C (n = 7)	NX-AL (n = 8)
Initial weight Day 0 (*g*)	121±10	121±11	123±10	119±11	118±11	120±10
Mid weight Day 14 (*g*)	184±15	184±15	182±14	181±12	180±8	179±12
Final weight Day 28 (*g*)	—	219±13	223±13	—	214±12	216±10
Total weight gain (*g*)	—	98±7	99±11	—	97±6	95±11
Creatinine clearance (*ml/min*)	—	1.7±0.5	1.6±0.6	—	0.7±0.1*‡	0.7±0.2*‡
Serum calcium (*mg/dl*)	—	9.7±0.4	9.3±0.3	—	9.8±0.4	10.1±0.4
Serum phosphorus (*mg/dl*)	—	7.1±0.4	7.3±1.0	—	6.9±0.4	6.6±0.5
Serum 25(OH)D (*ng/ml*)	—	50.2±22.1	45.1±17.3	—	68.4±12.7	45.6±20.0
Serum $1,25(OH)_2D$ (*pg/ml*)	—	67.7±36.5	68.5±10.2	—	61.4±26.6	64.0±30.7
Serum iPTH (*pg/ml*)	—	361±100	345±93	—	380±152	470±57

Values represent the mean±SD.
Days refer to day of the experiment (See Fig. 1).
* $P < 0.05$ vs. C.
‡ $P < 0.05$ vs. AL.

(23). Serum immunoreactive parathyroid hormone (iPTH) was measured using an antiserum (chick 12) directed against the carboxy terminus of the PTH molecule (24). Creatinine clearance was calculated using the conventional formula for clearance.

Statistical analysis. All values are expressed as the mean±SD. Statistical analysis of the data was done using the *t* test for unpaired samples, analysis of variance, and linear regression analysis (25).

Three nephrectomized control, one AL, and two NX-AL rats died during the experiment. These animals were excluded from all subsequent analysis.

Results

Initial body weight, final body weight, and weight gain during the experiment were similar among the four final groups (Table I). Moreover, the mean body weight at death for each basal group, Basal-C and Basal-NX, was not different from the measured weight for each respective final group on day 14. The creatinine clearances were reduced in subtotally nephrectomized animals. Renal function was similar, however, in C and AL intact rats, and in NX-C and NX-AL rats. The serum concentrations of calcium, phosphorus, iPTH, 25(OH)D, and $1,25(OH)_2D$ did not differ among the four final groups (Table I).

The results of the histologic measurements in bone for all six groups of rats, and the precision of these measurements, are summarized in Table II.

Total bone and matrix formation and periosteal bone and matrix formation were reduced in rats with normal renal function given repeated injections of aluminum (Fig. 3). Moreover, the rates of bone and matrix apposition at the periosteal surface fell in AL from their respective control values (Fig. 4). The mineralization lag time increased (Fig. 5), and the rates of periosteal osteoid maturation and initial mineralization decreased from control values in AL (Fig. 5). Despite these changes in mineralization lag time and osteoid maturation rate, no increase in osteoid seam width was observed in rats with normal renal function given aluminum (Table II).

In subtotally nephrectomized rats given aluminum, total bone and matrix formation decreased from the values measured in NX-C rats (Fig. 3); periosteal bone and matrix formation were similarly reduced. Moreover, although there were no differences between the two control groups, C and NX-C, in any of the measurements of bone formation, the values for total bone, total matrix, periosteal bone, and periosteal matrix formation were all less in NX-AL when compared with AL (Fig. 3).

The rates of periosteal bone and matrix apposition in NX-AL were below those measured in either NX-C or AL rats with normal renal function (Fig. 4). Furthermore, the mineralization lag time, osteoid maturation rate, and initial mineralization rate were each different from their respective values in NX-C and AL (Fig. 5). However, periosteal and endosteal osteoid widths were similar to control values in nephrectomized animals given aluminum (Table II).

The length of the endosteal resorption surface was similar in C and NX-C (Table III). After aluminum administration, resorption surface increased from control values in both AL and NX-AL. Moreover, the resorptive activity at the endosteal surface, measured as the linear rate of bone resorption, increased in NX-AL from the values determined in NX-C.

Discussion

The present results indicate that short-term aluminum administration substantially alters cortical bone growth in the rat. 4 wk of aluminum loading was associated with a 20% reduction in bone formation in rats with normal renal function and with a 40% reduction in animals which had undergone prior subtotal nephrectomy. Moreover, endosteal bone resorption increased after aluminum administration. No histologic evidence of osteomalacia was found, however, in either group of rats given aluminum. These findings in cortical bone differ from those of

Table II. Histologic Measurements in Final and Basal Rats and the Precision of these Measurements

	Basal-C (n = 10)	C (n = 10)	AL (n = 9)	Basal-NX (n = 10)	NX-C (n = 7)	NX-AL (n = 8)	Precision*
							%
Width (μm)							
Periosteal osteoid	6.1±0.5	5.5±0.7	5.3±0.5	5.6±0.6	4.7±1.0	4.9±0.6	±3
Endosteal osteoid	4.2±0.8	3.8±0.8	4.0±0.8	4.5±0.7	3.6±1.0	3.3±0.7	±4
Periosteal mineralization front	4.0±0.3	4.0±0.5	3.8±0.6	4.0±0.4	3.5±0.3	3.4±0.8	±4
Endosteal mineralization front	3.1±0.4	2.9±0.4	3.2±0.4	3.0±0.4	2.8±0.4	2.6±0.5	±4
Length (mm)							
Periosteal surface final	7.53±0.08	8.03±0.09	8.00±0.08	7.65±0.10	8.01±0.08	7.99±0.10	±1
initial	—	7.00±0.20	7.08±0.24	—	7.23±0.17	7.14±0.31	±1
Endosteal surface final	4.08±0.25	4.00±0.28	4.30±0.21	4.47±0.33	4.06±0.29	4.32±0.41	±2
initial	—	4.16±0.30	4.43±0.23	—	4.17±0.26	4.52±0.33	±2
Forming surface	2.57±0.29	2.66±0.41	2.60±0.34	2.78±0.47	2.90±0.51	2.49±0.63	±5
Resorbing surface	1.45±0.32	1.33±0.34	1.70±0.41	1.65±0.43	1.16±0.46	1.87±0.60	±7
Area (mm^2)							
Periosteal final	3.93±0.27	4.17±0.30	4.13±0.24	4.07±0.27	4.37±0.27	4.07±0.41	±1
initial	—	3.78±0.28	3.81±0.25	—	4.00±0.25	3.95±0.32	±1
Endosteal final	1.19±0.15	1.18±0.15	1.27±0.11	1.38±0.19	1.26±0.17	1.34±0.17	±2
initial	—	1.25±0.13	1.36±0.13	—	1.34±0.16	1.50±0.15	±2

Values represent the mean±standard deviation.
* Mean coefficient of variation for all groups from duplicate measurements on sections from individual rats.

two previous reports, both of which indicated that rats with renal insufficiency given repeated injections of aluminum chloride in daily dosages comparable to those used in the present study develop osteomalacia in trabecular bone (13, 14).

The duration of aluminum administration in the present study was 4 wk, whereas previous investigations have been 8–15 wk in length (12–14). This shorter time interval was chosen to examine the early effects of aluminum administration on bone. Although 4 wk may have been insufficient for the development of classic osteomalacic changes in these rats, substantial reductions in bone and matrix formation were found in intact, AL rats and in NX-AL animals. In preliminary studies

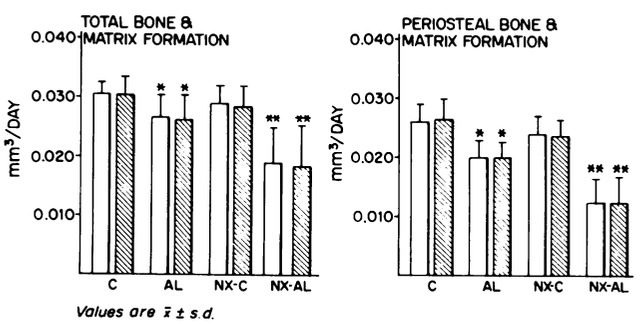

Figure 3. The rates of total bone (white bars) and matrix (striped bars) formation and of periosteal bone and matrix formation in C, AL, NX-C, and NX-AL rats. Bone and matrix formation were measured over a 14-d period using double tetracycline labeling of bone. Values are the mean±SD. *, $P < 0.05$ vs. C; **, $P < 0.001$ vs. NX-C.

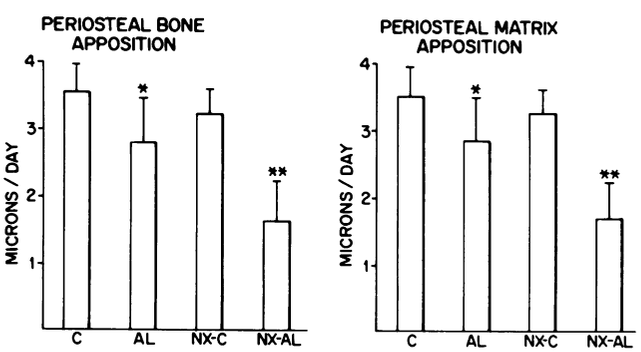

Figure 4. The rates of periosteal bone and matrix apposition in C, AL, NX-C, and NX-AL rats. The results represent the average width of new bone or matrix formed per day at the periosteal surface during the tetracycline labeling period. Values are the mean±SD. *, $P < 0.05$ vs. C; **, $P < 0.001$ vs. NX-C.

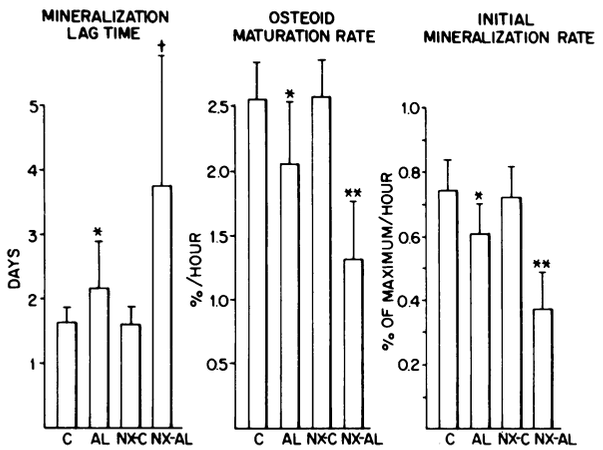

Figure 5. The mineralization lag time, the rate of osteoid maturation, and the rate of initial mineralization in C, AL, NX-C, and NX-AL rats. Values are the mean±SD. *, $P < 0.05$ vs. C; +, $P < 0.05$ vs. NX-C; **, $P < 0.001$ vs. NX-C.

of equal duration, a lesser daily dose of 2 mg/kg of elemental aluminum, in contrast to the dose of 2 mg/rat used in the present study, did not cause detectable changes in bone growth or histology as measured in this experimental model (Goodman, W. G., unpublished observations). Thus, the findings reported here most probably represent an early phase in the toxicity of aluminum in bone.

A feature common to both clinical and experimental evaluations of aluminum-associated osteomalacia has been a low rate of bone formation as measured by double tetracycline labeling (6–8, 14). The present results confirm this observation. Moreover, the current findings are similar to those reported in bone biopsy material from patients with early histologic evidence of aluminum-associated osteomalacia (7, 16). It has been suggested that impaired parathyroid hormone secretion may explain this state of low bone formation. Aluminum may accumulate in parathyroid tissue (26), and Morrissey et al. (17) have shown that aluminum reduces the secretion of iPTH from dispersed bovine parathyroid cells in vitro. The present results demonstrate that bone formation and apposition decrease early in the course of aluminum administration without concomitant reductions in the serum levels of iPTH. Although not conclusive, the determinations of iPTH were done using an assay which has been shown previously to be capable of discriminating between normal and low levels of the hormone in rats (24). Also, serum calcium and phosphorus concentrations did not change from control values in aluminum-treated rats, suggesting that PTH secretion was not substantially altered in these animals. Additional observations made in dogs given repeated parenteral injections of aluminum for 3–5 wk, which indicate no impairment in the secretion of iPTH in vivo, support this finding (15).

Preliminary results suggest that aluminum loading in dogs is associated with reduced serum levels of $1,25(OH)_2$ D (15, 27). Aluminum may also impair renal 1-alpha hydroxylase activity in rats (28). It is unlikely, however, that disturbances in vitamin D metabolism account for the present findings in bone. Not only were the serum calcium and phosphorus concentrations similar to control values in aluminum-treated animals, but also there were no differences among the four final groups in the serum levels of either 25(OH)D or $1,25(OH)_2D$. These results, and the lack of suppression of iPTH in AL and NX-AL, do not support a role for PTH or vitamin D in mediating the disturbances in bone formation observed in this and other studies. The current data are consistent, therefore, with a direct effect of aluminum to reduce new bone and matrix synthesis. The possibility remains, however, that changes in PTH secretion or vitamin D metabolism may develop during long-term exposure to aluminum, particularly in conjunction with renal insufficiency. Such disturbances could subsequently alter the early effects of aluminum on bone herein described.

Rats with normal renal function showed substantial reductions in bone and matrix formation during aluminum loading. Subtotal nephrectomy alone altered neither bone formation nor resorption in NX-C; these findings are consistent with the moderate degree of renal insufficiency observed and with the relatively short-term nature of the study. However, moderate renal insufficiency did accentuate the decreases in bone formation and

Table III. Indices of Endosteal Bone Resorption in Control and AL Rats

	C (n = 10)	AL (n = 9)	NX-C (n = 7)	NX-AL (n = 8)
Endosteal resorbing surface (*mm*)	1.33±0.34	1.70±0.42*	1.16±0.46	1.87±0.60‡
Linear rate of endosteal resorption (*μm/d*)	7.9±4.9	11.7±5.5	5.5±2.0	12.2±6.3‡

Values represent the mean±SD.
* $P < 0.05$ vs. C.
‡ $P < 0.05$ vs NX-C.

apposition observed during aluminum administration despite the comparable daily dosage given to rats in AL and NX-AL. The effect of nephrectomy, therefore, was not simply additive to that of aluminum. Since renal excretion is the primary route by which aluminum is removed from the body (10, 11), it is probable that renal insufficiency led to greater tissue retention during the period of aluminum administration in NX-AL when compared with AL. Although quantitation of aluminum in bone was not done in the present study, data previously reported in rats with impaired renal function given repeated injections of aluminum support this contention (13). Moreover, dogs receiving daily parenteral injections of aluminum show progressive tissue retention of the metal during continued aluminum exposure even in the presence of normal renal function (27, 29). Therefore, the accumulation of aluminum in tissues during aluminum loading most probably accounts not only for the reductions in bone formation observed in rats with normal renal function (AL) but also for the differences in bone growth between rats with normal (AL) and those with impaired renal function (NX-AL).

Several additional factors may explain the differences between the findings of the current study and those of previous investigators. First, all histologic measurements were made in cortical bone in contrast to earlier reports in which trabecular bone was examined (12–14). There are substantial differences between cortical and trabecular bone in the surface to volume ratio, in the rate of bone turnover, and in the response to different hormonal stimuli (30–32). Such differences may be critical in determining the skeletal response to physiological and experimental challenges. To date, osteomalacia has been described only in trabecular bone after experimental aluminum administration (12–14). Aluminum has been localized predominantly to the surface of trabecular bone by histochemical staining in experimental animals (14, 15) and by histochemical and electron microprobe techniques in human bone biopsy material. (6–9, 33). Such findings are consistent with the interpretation that the uptake of aluminum into bone is related to events at the bone surface. Thus, trabecular bone, by virtue of both its higher surface to volume ratio and its greater rate of turnover, may be more susceptible than cortical bone to the toxic effects of aluminum. Although preliminary, data from our laboratory suggest that the histological response to short-term aluminum loading in trabecular bone may indeed be different than that observed in the tibial cortex of the rat (34).

Second, nutritional considerations are important in any study of bone growth (35–38). Protein-calorie malnutrition impairs new bone formation and bone collagen synthesis (35–37). Rats from each of the four groups in the present investigation were given equal amounts of food and exhibited comparable weight gains over the course of the experiment. Therefore, differences in bone growth among these groups cannot be attributed to alterations in nutritional status. In contrast, previous reports of bone growth and bone histology in rats studied for periods as long as 8–15 wk indicate that aluminum-treated animals gain less weight than saline-injected control animals (12–14). Thus, the disturbances in bone growth and mineralization observed in these earlier studies may, in part, be explained by changes in nutritional factors as a consequence of aluminum administration.

Osteomalacia is characterized by widened osteoid seams, an increase in the width of the mineralization front, a delay in the onset of mineralization, and a reduced rate of calcification in newly formed osteoid (19). The calculated results for mineralization lag time, osteoid maturation rate, and initial mineralization rate suggest both a delay in the onset of mineralization in newly formed bone and a reduction in the rate of mineralization in rats given aluminum (Fig. 5). However, the measurements of osteoid seam width and mineralization front width, which did not increase from control values in either AL or NX-AL, fail to support these observations. It must be noted that the percent change in each of the above calculated variables was comparable with the measured change in bone and matrix apposition for each experimental group, i.e., 20% for AL and 40% for NX-AL. In contrast, the classic state of impaired osteoid maturation and mineralization, vitamin D-deficient osteomalacia, is characterized by greater reductions in bone apposition than in matrix apposition (19). This results in widened osteoid seams. The parallel reductions in bone and matrix apposition observed in AL and NX-AL, and the lack of osteoid accumulation in either group, indicate that the changes in mineralization lag time, osteoid maturation rate, and initial mineralization rate were all consistent with and appropriate for the rates of bone and matrix apposition measured. This interpretation is supported by observations made in normal rats growing at different rates that document that the calculated normal values for these three processes are dependent upon the absolute rates of apposition of bone and matrix (Goodman, W. G., unpublished observations). The close agreement between the regression lines for intact, control animals and for the pooled data from all four study groups from the present experiment suggest that the administration of aluminum did not substantially alter the normal relationship between the measured rates of bone and matrix apposition and the calculated variables of mineralization lag time, osteoid maturation rate, and initial mineralization rate (Table IV). Although these data do not exclude the possibility of a subtle, early defect in the maturation of osteoid, they do indicate that, if present, such an abnormality is indeed minor when compared with the reductions in bone formation and apposition described. Thus, the maturation of osteoid and the initial phases of mineralization are not disturbed during short-term exposure to aluminum. Although it has been suggested that aluminum deposition at the mineralization front may interfere with calcification and lead to osteoid accumulation (9), the present data do not support this contention. Rather, the primary effect of aluminum on cortical bone in the rat is to suppress matrix and bone synthesis.

Endosteal resorption surface increased in AL and in NX-AL, and resorptive activity at the endosteum was enhanced in

Table IV. Correlation Analysis for Control Rats and for All Four Experimental Groups

Variable	Population	Y intercept	Slope	r
Mineralization lag time	Control (n = 10)	2.88	−0.35	−0.68
vs. matrix apposition	Study group* (n = 34)	6.02‡	−1.3	−0.82
Osteoid maturation rate	Control (n = 10)	0.11	0.69	0.88
vs. matrix apposition	Study group* (n = 34)	0.10	0.71	0.74
Rate of initial				
mineralization vs.	Control (n = 10)	0.12	0.18	0.77
bone apposition	Study group* (n = 34)	0.04	0.20	0.97

* Pooled data for C, AL, NX-C, NX-AL.
‡ $P < 0.05$ compared with control.

NX-AL. Few data are available regarding the effect of aluminum on bone resorption either in vitro or in vivo. Chan et al. (13) found an increase in the number of osteoclasts and in the extent of resorptive surfaces in the trabecular bone of uremic rats given aluminum, results that are consistent with the present findings. Other investigators have reported evidence of an increase in acid and alkaline phosphatase activity in rat calvaria in tissue culture during exposure to low concentrations of aluminum (39). Further study will be required to confirm these observations and to clarify the effect of aluminum on bone resorption in general and on the cellular activity of osteoclasts in particular.

In summary, short-term aluminum administration reduces new bone and matrix formation in the absence of either growth retardation or changes in the serum levels of iPTH or metabolites of vitamin D. Whether these disturbances in bone and matrix formation influence the subsequent uptake of aluminum at bone-forming surfaces and/or lead to histologic osteomalacia cannot be determined from the present data. The results support the contention that aluminum is toxic to bone, but suggest that either more prolonged exposure to this metal or additional factors that affect bone metabolism may be required to induce osteomalacia in cortical bone. Aluminum may also enhance bone resorption and therefore contribute to osteopenia in clinical states associated with the accumulation of aluminum in bone.

Appendix

The cross-sections of the tibial diaphysis, on which histologic measurements are made, are in the configuration of an annulus. Thus, to calculate osteoid and mineralization front areas, formulae for determining the area of an annulus (Eq. A) and the area of a segment of an annulus (Eq. B) are used,

$$W(Li + \pi W) = A = W(Lo - \pi W), \quad (A)$$

$$WLs/Li(Li + \pi W) = A = WLs/Lo(Lo - \pi W), \quad (B)$$

where A is area, W is width, Li and Lo are internal and external circumferences, respectively, and Ls is the length of a segment of a circumference. This approach is supported by observations that actual measurements of area in these sections closely approximate those calculated assuming that the circumference of the section is a circle.

The calculations used to determine bone formation and resorption in individual rats are given below. All variables are measured in rats from the final groups after double tetracycline labeling of bone, except as denoted by the subscript b, which indicates measurements made in basal rats. All measurements are expressed in millimeters for length, square millimeters for area, and cubic millimeters for volume unless otherwise specified.

Area of periosteal bone-final (Apf). The area of mineralized bone formed at the periosteum during the time interval between the first and second tetracycline labels, as demarcated by the inner border of the initial periosteal tetracycline label (IPA) and the border of mineralized bone, excluding osteoid, at the periosteal surface (PA), and measured in final rats is represented as

$$Apf = PA - IPA. \quad (1)$$

This measurement will include the area of the existing mineralization front at the start of the bone labeling period into which tetracycline diffuses passively, but which does not represent new bone formation during this period.

Area of periosteal bone-basal (Apb). The Apb is the area occupied by the periosteal mineralization front at the time of administration of the initial tetracycline label, and determined from measurements in basal rats, where PMF_b and PS_b are the periosteal mineralization front width and the length of the periosteal surface, respectively. The width of the mineralization front is determined from measurements of the width of the band of tetracycline fluorescence immediately adjacent to the surface osteoid seam. Apb is calculated using Eq. A.

$$Apb = PMF_b(PS_b - \pi PMF_b). \quad (2)$$

Area of periosteal bone formation (Apbf). The true area of periosteal bone formed during the bone labeling period corrected for the area of the initial periosteal mineralization front present at the start of the period is represented by

$$Apbf = Apf - Apb. \quad (3)$$

Rate of periosteal bone formation (Rpbf). Rpbf is the volume of new bone formed per unit time, in cubic millimeters per day, at the periosteal surface, where T represents the duration of the bone labeling period in days, i.e., the time interval (T) between the initial dose of tetracycline and death for rats in the final groups.

$$Rpbf = Apbf/T = (Apf - Apb)/T. \quad (4)$$

Area of endosteal bone-final (Aef). The Aef is the area of bone formed at the endosteum during the bone labeling period and analogous to Apf,

$$\text{Aef} = \text{IEA} - \text{EA}, \tag{5}$$

where EA is the area enclosed by the endosteal surface, exclusive of osteoid, and IEA is the area enclosed by the outer edge of the initial endosteal tetracycline label.

Area of endosteal bone-basal (Aeb). This is the area of the existing endosteal mineralization front at the beginning of the labeling period into which tetracycline diffuses, and is analogous to Apb.

$$\text{Aeb} = \text{EMF}_b\ \text{FS}_b/\text{ES}_b\ (\text{ES}_b + \pi\text{EMF}_b) \tag{6}$$

It is calculated using Eq. B, where EMF_b is the width of the basal endosteal mineralization front, FS_b is the length of the basal endosteal forming surface, and ES_b is the total length of the basal endosteal surface.

Area of endosteal bone formation (Aebf). The area of new bone formed at the endosteum during the interval between tetracycline labels, and corrected for the area of the mineralization front present at the beginning of the labeling period is represented by

$$\text{Aebf} = \text{Aef} - \text{Aeb}. \tag{7}$$

Rate of endosteal bone formation (Rebf). The volume of new bone formed at the endosteum per unit time, in cubic millimeters per day.

$$\text{Rebf} = \text{Aebf}/T = (\text{Aef} - \text{Aeb})/T \tag{8}$$

Rate of total bone formation (Rtbf). Rtbf is the daily rate of new bone formation, and expressed in cubic millimeters per day; the sum of the rates of periosteal and endosteal bone formation.

$$\text{Rtbf} = \text{Rpbf} + \text{Rebf} = (\text{Apf} - \text{Apb} + \text{Aef} - \text{Aeb})/T. \tag{9}$$

Rate of total matrix formation (Rtmf). Bone matrix (osteoid) must be deposited and undergo mineralization to form new bone. Thus, matrix formation can be derived from the sum of the amount of new bone formed per unit time, i.e., Rtbf, and the net increase or decrease per unit time in the total area of osteoid during the bone labeling period. This includes all matrix formed whether mineralized or not. Thus,

$$\text{Rtmf} = \text{Rtbf} + (\text{Aof} - \text{Aob})/T, \tag{10}$$

where Aof and Aob are the total osteoid areas from final and basal rats, respectively. Aof and Aob are calculated using Eqs. A and B as follows:

$$\text{Aof} = \text{POW}(\text{PS} - \pi\text{POW}) + \text{EOW}\ \text{FS}/\text{ES}\ (\text{ES} + \pi\text{EOW}) \tag{11}$$

$$\text{Aob} = \text{POW}_b(\text{PS}_b - \pi\text{POW}_b) + \text{EOW}_b\ \text{FS}_b/\text{ES}_b\ (\text{ES}_b + \pi\text{EOW}_b), \tag{12}$$

where POW and EOW are the periosteal and endosteal osteoid seam widths, respectively, PS is the length of the periosteal surface, ES is the length of the endosteal surface, and FS is the length of the endosteal-forming surface.

Periosteal bone apposition rate (Rpba). This is a measure of the width of mineralized bone, in microns per day, deposited along the length of the periosteal surface; it is calculated by dividing the periosteal bone formation rate by the average length of periosteal-forming surface during the interval between the initial and final tetracycline labels. Thus,

$$\text{Rpba} = (\text{Apf} - \text{Apb})/T \times 2/(\text{PS} + \text{IPS}), \tag{13}$$

where PS is the length of the periosteal surface and IPS is the length of the initial periosteal tetracycline label. Bone apposition can be calculated similarly at the endosteum.

Periosteal matrix apposition rate (Rpma). This represents the width of new matrix deposited, in microns per day, at the periosteal surface and is analogous to Rpba. It is calculated by adding the daily increment or decrement in the width of the periosteal osteoid seam to the bone apposition rate. Thus,

$$\text{Rpma} = \text{Rpba} + (\text{POW} - \text{POW}_b)/T, \tag{14}$$

where POW and POW_b are the osteoid seam widths from the final and basal rats, respectively. Matrix apposition is calculated at the endosteal surface in a similar fashion.

Mineralization lag time (Tm). Newly formed matrix (osteoid) must undergo a series of changes before calcification can begin. The mineralization lag time is a measure of the length of this interval, expressed in days, and is calculated by dividing the mean osteoid seam width over the course of the bone labeling period by the rate of matrix apposition. Tm can be derived at both the periosteum (Tmp) and at the endosteum (Tme). Thus,

$$\text{Tm} = (\text{OW} + \text{OW}_b)/2\text{Rma}, \tag{15}$$

where OW and OW_b represent the final and basal osteoid seam widths, where Rma is the rate of matrix apposition, and where each is measured at either the periosteum or the endosteum.

Osteoid maturation rate (Ro). This is a measure of the rate at which changes occur in osteoid in preparation for the onset of calcification. Based on the concept that osteoid is 0% mature when initially deposited and 100% mature when mineralization begins, osteoid maturation can be expressed in percentage per hour and can be determined at both the periosteum (Rop) and at the endosteum (Roe). Thus,

$$\text{Ro} = 100/\text{Tm} \times 24, \tag{16}$$

where Tm is the mineralization lag time at either the periosteum or the endosteum.

Rate of initial mineralization (Rm). By refractive index measurements and by electron microprobe analysis, the maximum concentration of calcium within the mineralization front is 20% of that in mineralized cortical bone, and this concentration is achieved near the junction between the mineralization front and more fully calcified bone. Therefore, the rate at which this concentration of calcium, C = 0.2, is reached within the mineralization front can be stated as the rate of initial mineralization. It is calculated by dividing the bone apposition rate by the mean mineralization front width over the duration of the labeling period, and is expressed as percentage of maximum per hour. Rm is determined at both the periosteal (Rmp) and endosteal (Rme) surfaces. Thus,

$$\text{Rm} = 2\text{CRba}/(\text{MF} + \text{MF}_b) \times 100/24, \tag{17}$$

where C is the constant 0.2, MF and MF_b are the widths of the mineralization front in final and basal rats, respectively, Rba is the rate of bone apposition, and where all are measured at either the periosteum or the endosteum.

Rate of endosteal bone resorption (Rebr). Rebr is the volume of bone reabsorbed per unit time at the endosteum, in cubic millimeters per day. It represents the total resorption rate since no reabsorption occurs at the periosteum, and is calculated as the sum of the difference between the endosteal areas in individual final (EA) and basal (EA_b) rats, compared on the basis of rank, and the area of endosteal bone formation (Aebf) as determined in the final rats.

$$\text{Rebr} = (\text{EA} - \text{EA}_b + \text{Aebf})/T. \quad (18)$$

Rate of linear bone resorption (Rlbr). Rlbr is the width of endosteal bone reabsorbed, in microns per day, along the length of the endosteal resorbing surface. It is calculated by dividing the area of bone reabsorbed per day (Rebr) by the mean length of the endosteal resorbing surface over the labeling period. Thus,

$$\text{Rlbr} = 2\text{Rebr}/(\text{RS} + \text{RS}_b), \quad (19)$$

where RS and RS_b are the lengths of the endosteal resorbing surface in final and basal rats, respectively.

Acknowledgments

The authors wish to express their gratitude to Dr. D. J. Baylink and his laboratory staff for their generous assistance in establishing the techniques employed to study the rat model used in these studies in our laboratory. We also recognize the excellent technical assistance of Mr. Arch Taylor of Dr. Baylink's laboratory for the measurements of serum iPTH. Drs. C. K. Abrass, J. W. Coburn, and Donald Whedon provided numerous helpful comments and suggestions during the preparation of the manuscript. Ms. Gigi Yapo provided expert secretarial assistance.

Dr. Baylink was supported by a grant from the National Institutes of Health, AM-31062.

References

1. Platts, M. M., G. C. Goods, and J. S. Hislop. 1977. Composition of the domestic water supply and the incidence of fractures and encephalopathy in patients on home dialysis. *Br. Med. J.* 2:657–660.

2. Ward, M. K., T. G. Feest, H. A. Ellis, I. S. Parkinson, and D. N. S. Kerr. 1978. Osteomalacia and dialysis osteodystrophy: evidence for a water-borne etiological agent, probably aluminum. *Lancet.* I:841–845.

3. Parkinson, I. S., T. G. Feest, M. K. Ward, R. W. P. Fawcett, and D. N. S. Kerr. 1979. Fracturing dialysis osteodystrophy and dialysis encephalopathy: an epidemiological survey. *Lancet.* I:406–409.

4. Pierides, A. M., W. G. Edwards, Jr., U. S. Cullu, Jr., J. T. McCall, and H. A. Ellis. 1980. Hemodialysis encephalopathy with osteomalacic fractures and muscle weakness. *Kidney Int.* 18:115–124.

5. Drueke, T. 1980. Dialysis osteomalacia and aluminum intoxication. *Nephron.* 26:207–210.

6. Hodsman, A. B., D. J. Sherrard, A. C. Alfrey, S. Ott, A. S. Brickman, M. L. Miller, N. A. Maloney, and J. W. Coburn. 1982. Bone aluminum and histomorphometric features of renal osteodystrophy. *J. Clin. Endocrinol. Metab.* 54:539–546.

7. Ott, S. M., N. A. Maloney, J. W. Coburn, A. C. Alfrey, and D. J. Sherrard. 1982. The prevalence of aluminum in renal osteodystrophy and its relationship to response to calcitriol therapy. *N. Engl. J. Med.* 307:709–713.

8. Boyce, B. F., G. S. Fell, H. Y. Elder, B. J. Junor, H. L. Elliot, G. Geastall, I. Fogelman, and I. T. Boyle. 1982. Hypercalcaemic osteomalacia due to aluminum toxicity. *Lancet.* II:1009–1013.

9. Maloney, N. A., S. M. Ott, A. C. Alfrey, N. L. Miller, J. W. Coburn, and D. J. Sherrard. 1982. Histological quantitation of aluminum in iliac bone from patients with renal failure. *J. Lab. Clin. Med.* 99:206–216.

10. Kovalchik, M. T., W. D. Kaehny, A. P. Hegg, J. T. Jackson, and A. C. Alfrey. 1978. Aluminum kinetics during hemodialysis. *J. Lab. Clin. Med.* 92:712–720.

11. Alfrey, A. C., A. Hegg, and P. Craswell. 1980. Metabolism and toxicity of aluminum in renal failure. *Am. J. Clin. Nutr.* 33:1509–1516.

12. Ellis, H. A., J. H. McCarthy, and J. Herrington. 1979. Bone aluminum in hemodialysed patients and in rats injected with aluminum chloride: relationship to impaired bone mineralization. *J. Clin. Pathol.* 32:832–834.

13. Chan, Y., A. C. Alfrey, S. Posen, D. Lissner, E. Hills, C. Dunstan, and R. Evans. 1983. Effect of aluminum on normal and uremic rats: tissue distribution, vitamin D metabolites, and quantitative bone histology. *Cal. Tiss. Int.* 23:344–351.

14. Robertson, J., A. Felsenfeld, C. Haygood, and F. Llach. 1983. An animal model of aluminum induced osteomalacia: role of chronic renal failure and parathyroid hormone. *Kidney Int.* 23:327–335.

15. Goodman, W. G., D. A. Henry, R. Horst, R. K. Nudelman, A. C. Alfrey, and J. W. Coburn. 1984. Parenteral aluminum administration in the dog. II. Induction of osteomalacia and effect on vitamin D metabolism. *Kidney Int.* In press.

16. Hodsman, A. B., D. J. Sherrard, E. G. C. Wong, A. S. Brickman, D. B. N. Lee, A. C. Alfrey, F. R. Singer, A. W. Norman, and J. W. Coburn. 1981. Vitamin D resistant osteomalacia in hemodialysis patients lacking secondary hyperparathyroidism. *Ann. Int. Med.* 94:629–637.

17. Morrissey, J., M. Rothstein, G. Mayor, and E. Slatopolsky. 1983. Suppression of parathyroid hormone secretion by aluminum. *Kidney Int.* 23:699–704.

18. Frost, H. M. 1963. Measurement of human bone formation by means of tetracycline labelling. *Can. J. Biochem. Phys.* 41:31–38.

19. Baylink, D. J., M. Stauffer, J. Wergedal, and C. Rich. 1970. Formation, mineralization, and resorption of bone in vitamin D deficient rats. *J. Clin. Invest.* 49:1122–1134.

20. Willis, J. B. 1960. The determination of metals in blood serum by atomic absorption spectroscopy. I. Calcium. *Spectrochim. Acta Part A Mol. Spectrosc.* 16:259–272.

21. Fiske, C. H., and H. Y. Subbarow. 1925. The colorimetric determination of phosphorous. *J. Biol. Chem.* 66:375–400.

22. Heinegard, D., and G. Tidestrom. 1973. Determination of serum creatinine by a direct colorimetric method. *Clin. Chem. Acta.* 43:305–311.

23. Horst, R. L., E. T. Littledike, J. L. Riley, and J. L. Napoli. 1981. Quantitation of vitamin D and its metabolites and their plasma concentrations in five species of animals. *Ann. Biochem. Exp. Med. (Calcutta).* 116:189–203.

24. Chertow, B. S., D. J. Baylink, J. E. Wergedal, M. H. H. Su, and A. W. Norman. 1975. Decrease in serum immunoreactive parathyroid hormone in rats and in parathyroid hormone secretion in vitro by 1,25-dihydroxycholecalciferol. *J. Clin. Invest.* 56:668–678.

25. W. J. Dixon and F. J. Massey, editors. 1969. Introduction to statistical analysis. McGraw Hill Book Co., New York. 75–94, 150–193.

26. Cann, C. E., S. G. Prussin, and G. S. Gordan. 1979. Aluminum uptake by the parathyroid glands. *J. Clin. Endocrinol. Metab.* 49:543–545.

27. Henry, D. A., W. G. Goodman, R. K. Nudelman, N. D. DiDomenico, A. C. Alfrey, E. Slatopolsky, T. M. Stanley, and J. W. Coburn. 1984. Parenteral aluminum administration in the dog: I. Plasma kinetics, tissue distribution, and effects on calcium metabolism and parathyroid hormone. *Kidney Int.* In press.

28. Smothers, R. L., H. Kawashima, J. W. Coburn, and K. Kurokowa. 1983. Effect of aluminum administration on 25-hydroxyvitamin D3-1a-hydroxylase in the rat kidney. Proceedings of the Fifth Annual Scientific Meeting, American Society for Bone and Mineral Research, San Antonio, Texas, June 5–7. A-67.

29. DiDomenico, N. D., D. A. Henry, R. K. Nudelman, N. L. Miller, A. C. Alfrey, W. G. Goodman, and J. W. Coburn. 1982. Aluminum kinetics and distribution in the dog. *Kidney Int.* 21:271.

30. Byers, P. D. 1977. The diagnostic value of bone biopsies. *In* Metabolic Bone Disease. S. M. Krane and L. V. Avioli, editors. Academic Press, Inc., New York. I:184–236.

31. Parfitt, A. M. 1976. The actions of parathyroid hormone on bone. Relation to bone remodeling and turnover, calcium homeostasis, and metabolic bone disease. I. *Metab. Clin. Exp.* 25:809–844.

32. Riggs, B. L., H. W. Wahner, W. L. Dunn, R. B. Mazess, K. P. Offord, and L. J. Melton. 1981. Differential changes in bone mineral density of the appendicular and axial skeleton with aging: relationship to spinal osteoporosis. *J. Clin. Invest.* 67:328–335.

33. Cournot-Witmer, G., J. Zingraff, J. J. Plachot, F. Escaig, R. Lefevre, P. Boumati, A. Bourdeau, M. Garabedian, P. Galle, R. Bourdon, T. Drueke, and S. Balsan. 1981. Aluminum localization in bone from hemodialyzed patients: relationship to matrix mineralization. *Kidney Int.* 20:375–385.

34. Goodman, W. G., and J. Gilligan. 1983. Differential effects of aluminum administration on cortical and trabecular bone. Proceedings of the Fifth Annual Scientific Meeting, American Society for Bone and Mineral Research, San Antonio, Texas, June 5–7. A-34.

35. El-Maraghi, N. R. H., B. S. Platt, and R. J. C. Stewart. 1965. The effect of the interaction of dietary protein and calcium on the growth and maintenance of the bones of young, adult, and aged rats. *Br. J. Nutr.* 19:491–509.

36. Jha, G. J., M. G. Deo, and V. Ramalingaswami. 1968. Bone growth in protein deficiency. *Am. J. Path.* 53:1111–1121.

37. Le Roith, D., and B. L. Pimstone. 1973. Bone metabolism and composition in the protein-deprived rat. *Clin. Sci. (Lond.).* 44:305–319.

38. Shires, R., L. V. Avioli, M. E. Bergfeld, M. D. Fallon, E. Slatopolsky, and S. L. Teitelbaum. 1980. Effects of semistarvation on skeletal homeostasis. *Endocrinology.* 107:1530–1535.

39. Lieberherr, M., B. Grosse, L. Cornot-Witmer, C. L. Thil, and S. Balsan. 1982. *In vitro* effects of aluminum on bone phosphatases: a possible interaction with bPTH and vitamin D3 metabolites. *Cal. Tiss. Int.* 34:280–284.